ISIJ International, Vol. 44 (2004), No. 8, pp. 1431–1440

Role of Combined Addition of Niobium and Boron and of Molybdenum and Boron on Hardnenability in Low Carbon Steels

Takuya HARA, Hitoshi ASAHI, Ryuji UEMORI[1)] and Hiroshi TAMEHIRO[2)]

Nippon Steel Corporation, Steel Research Laboratories, 20-1 Shintomi, Futtsu, Chiba 293-8511 Japan.
1) Nippon Steel Corporation, Kimitsu R&D Laboratories, 1-1 Kimitsu, Kimitsu, Chiba 299-1141 Japan.
2) Chiba Institute of Technology, Department of Materials Science, 2-17-1 Tsudanuma, Narashino, Chiba 275-0016 Japan.

(*Received on March 15, 2004; accepted in final form on May 25, 2004*)

Effects of the combined addition of niobium (Nb) and boron (B) and of molybdenum (Mo) and B on hardenability were investigated using low carbon steels. Strength synergically increases due to the combined addition of Nb and B and that of Mo and B. It is thought that strength increases due to these combined additions because austenite (γ) to ferrite (α) transformation is retarded and bainite transformation is promoted due to the increase in the segregated B along the γ grain boundary before γ to α transformation. The mechanism for the increase in the segregated boron along the γ grain boundary by these combined additions is considered below. $Fe_{23}(C, B)_6$ precipitates formed along the γ grain boundary are suppressed by these combined additions because of the suppression of C diffusion towards the γ grain boundary due to the precipitation of the fine dispersive niobium-titanium carbonnitride (Nb, Ti)(C, N) or titanium-molybdenum carbonnitride (Ti, Mo)(C, N) and the formation of C clusters of Nb and Mo during rolling or during cooling after rolling. Therefore, the segregated B along the γ grain boundary increases and γ to α transformation is retarded. The combined addition of Nb and B or that of Mo and B in low C bainitic steel is effective for increasing strength without deteriorating low temperature toughness. It is clarified that the increments of hardenability by the combined addition of Nb and B is different from that of Mo and B due to the difference of the amount of carbide precipitates.

KEY WORDS: low carbon bainite; boron; niobium; molybdenum; γ to α transformation; combined additions.

1. Introduction

Much research on the effect of B has been carried out and published. For example, it is well known that hardenability remarkably increases through the addition of boron.[1–8)] Moreover, B has been utilized in controlled-rolled steels. Low C bainitic steels and ultra low C bainitic steels have been developed.[9–13)] Adding Nb and B is an effective way to achieve a good balance of strength and low temperature toughness in Thermo-Mechanical Controlled Process (TMCP) plates. Much research on low C bainitic steels, especially the combined addition of Nb and B, has been carried out, and manufacturing technology on these steels up to 30 mm thickness used for large diameter linepipes was developed.[9–13)] The role of the combined addition of Nb and B was investigated and summarized as follows. The recrystallization stop temperature of γ is elevated by the combined addition of Nb and B. Coarse B precipitates $Fe_{23}(CB)_6$ were suppressed and the segregated B increased along the γ grain boundary, as a results, γ to α transformation is suppressed. It is assumed that the coarse B precipitates, that is $Fe_{23}(CB)_6$, are suppressed because strain induced precipitation of niobium carbide (NbC) or titanium carbide (TiC) reduces the supply of C required for these precipitates.[14)]

Hardenability due to the combined addition of Mo and B was also investigated by Karlsson *et al.*[15)] and one of the authors.[16–18)] Hardenability by the combined addition of Mo and B synergically increases. However, few researches have been carried out on hardenability due to combined addition of Nb and B and that of Mo and B in low C steels. The purpose of this study is to clarify the role of these combined additions on hardnenability in low carbon steels and to make clear the reasons of remarkable increase in hardenability for the combined additions from the viewpoint of the precipitates along the prior γ grain boundary and in the prior γ grain.

2. Experimental Procedure

2.1. Material

Table 1 shows the chemical compositions of used steels. Low C aluminum (Al) killed steels were used in order to obtain the bainite microstructure by adding alloying elements, such as Nb, Mo and B. The steels with single addition and combined addition of Nb, Mo and B, of which base chemical composition is 0.015%C–0.20%Si–1.5%Mn–0.020%Al–0.015%Ti–0.0020%N (mass%), were melted using a 300 kg vacuum induction melting furnace (VIM) in a laboratory and cast into 100 kg ingots. The ingot size was 160 mm in thickness, 140 mm in width, and 300 mm in length. Six ingots were reheated at 1 200°C for 1 h and controlled-rolled between 880 and 800°C, then air

Table 1. Chemical compositions of laboratory melted steels (mass%, * ppm).

Steel	C	Si	Mn	P*	S*	Mo	Nb	Ti	Al	B*	N*	O*
Base	0.014	0.20	1.54	<20	6	—	—	0.015	0.020	—	21	12
B steel	0.014	0.20	1.54	<20	6	—	—	0.015	0.020	8	21	11
Nb steel	0.015	0.20	1.52	<20	6	—	0.040	0.015	0.021	—	22	18
Nb-B steel	0.014	0.20	1.54	<20	6	—	0.037	0.015	0.020	9	23	10
Mo steel	0.015	0.21	1.53	<20	6	0.35	—	0.014	0.023	—	21	14
Mo-B steel	0.015	0.21	1.54	<20	6	0.35	—	0.013	0.022	8	23	13

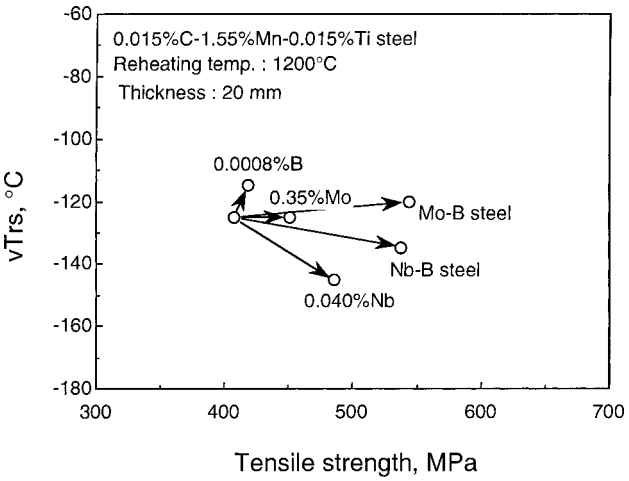

Fig. 1. Relationship between Charpy impact transition temperature and strength.

cooled to room temperature. An average cooling rate in the mid-thickness between 800 and 500°C was 20°C/s. The cumulative reduction below 880°C was 80%.

2.2. Mechanical Properties

Mechanical properties were examined by using full-thickness rectangular tensile specimens in the longitudinal direction and full-size 2 mm V-notch Charpy impact specimens in the transverse direction in order to evaluate the effect of alloying elements such as Nb, Mo and B on the balance of strength and low temperature toughness.

2.3. Transformation Behavior after Hot Working

Transformation behavior after hot working was measured using a hot-rolling simulator. The cylindrical specimens, which were 8 mm in diameter and 12 mm long, were taken from the mid-thickness. Specimens were worked with 15% reduction twice at 850°C after being reheated at 1 200°C for 20 min and then cooled by Helium (He) gas (The cooling rate was approximately 60°C/s). The strain rate was 10/s and the interpass time was 10 s. The effect of cooling rate after reduction on transformation behavior was also investigated in comparison with γ to α transformation behavior of 20 mm thick rolled plates.

2.4. Microstructure and Precipitates Analysis

Microstructure was observed by a scanning electron microscope (SEM). The distribution of B was observed by the α-ray track etching (ATE) method.[19–21] B content as precipitates was measured on the residue prepared by electrolytic extraction. Precipitates along a prior γ grain boundary and those in a prior γ grain were identified using a transmission electron microscope (TEM) and an atom probe field ion microscope (AP-FIM). TEM observation was performed on an extraction replica after electrolytic etching. Precipitates were identified by analysis of electron beam diffraction pattern and energy dispersive X-ray spectroscopy (EDS) analysis. The needle specimen of AP-FIM, of which the radius of top curvature was 50 nm, was made by electropolishing. The electropolishing solution was chromic acid saturated with phosphoric acid. Ne gas was used as image gas. Pulse fraction was 16% and its frequency was 250 Hz.[22,23]

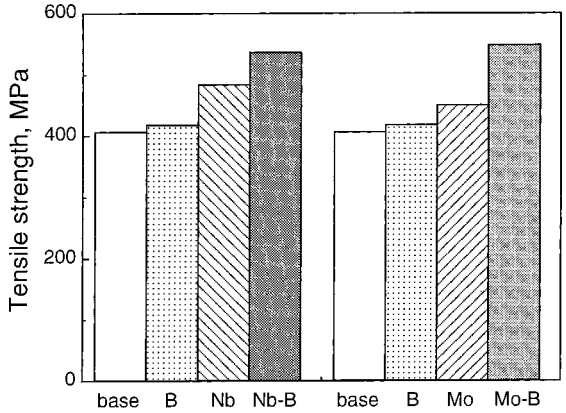

Fig. 2. Effect of the combined addition of niobium and boron or molybdenum and boron on tensile strength.

3. Results

3.1. Mechanical Properties and Microstructure of 20 mm Thick Plates

3.1.1. Relationship between Strength and Low Temperature Toughness

The relationship between strength and Charpy impact transition temperature (vTrs) was plotted in **Fig. 1**. Tensile strengths were in the range of 400 to 550 MPa. Strength increases in the order of single addition of B (B steel), Mo (Mo steel), Nb (Nb steel), the combined addition of Nb and B (Nb–B steel) and of Mo and B (Mo–B steel). Tensile strength drastically increased for Nb–B steel and Mo–B steel. Nb addition tended to decrease vTrs and B addition increased vTrs. The vTrs of Nb and Nb–B steels were −145 and −135°C, respectively and were extremely low. The single addition of Mo steel did not change the vTrs, however, the combined addition of Mo and B slightly increased vTrs as compared with the base steel. But, the vTrs was very low of −120°C. The vTrs of Mo–B steel was 10°C higher than that of Mo steel. The reason was supposed to be the large increase in tensile strength due to the combined additions. **Figure 2** shows the effect of the combined addition of Nb and B and that of Mo and B on tensile strength. The increase in strength due to the combined addition of Nb and B was greater than the summation of increases in strength due to the single additions of Nb and B. The increase in strength due to the combined addition of Mo and B was also larger than the summation of increases in strength due to the single addition of Mo and B. The tensile strengths increased by 80 and 130 MPa by the single

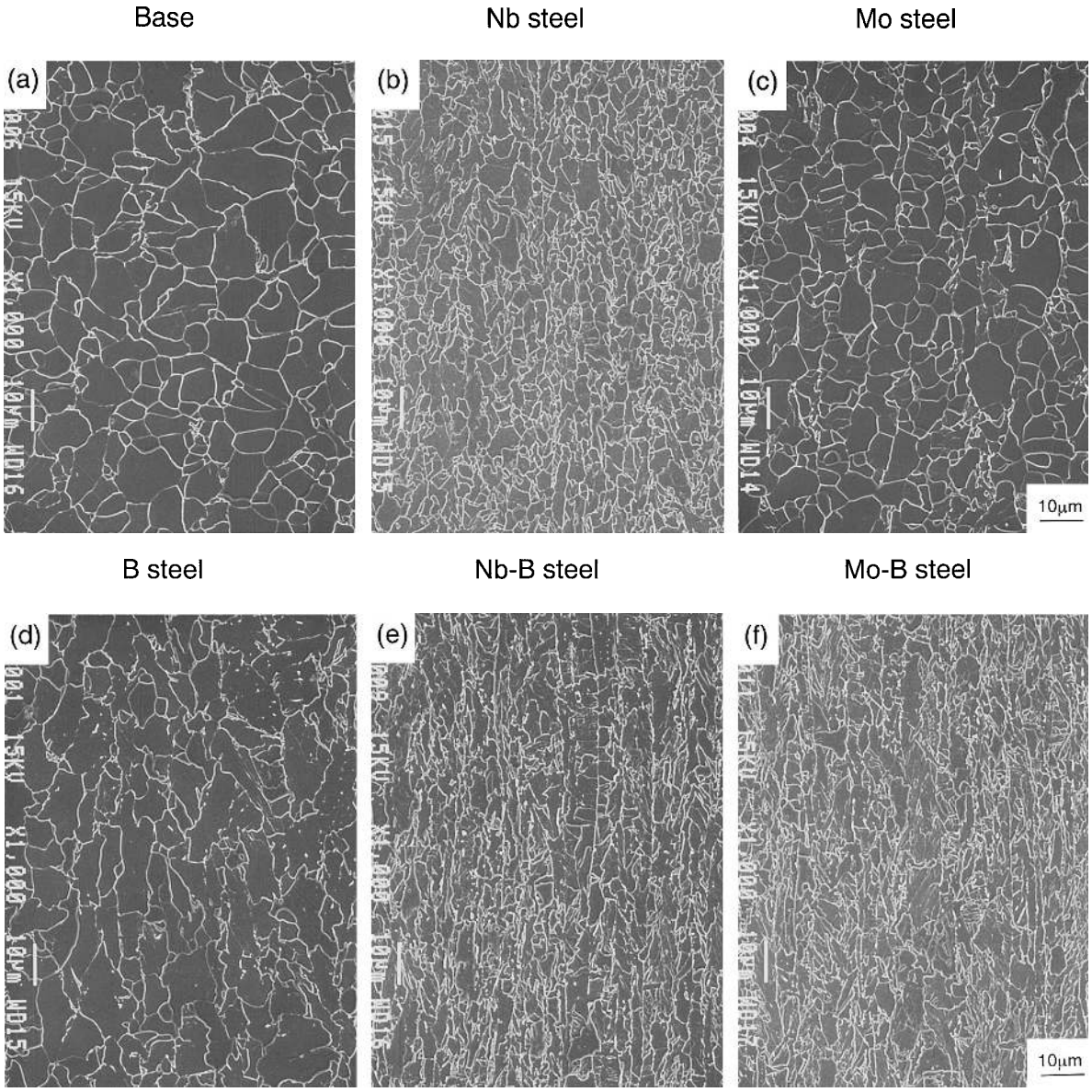

Fig. 3. Scanning electron micrographs of 20 mm thick plates.

addition of Nb and the combined addition of Nb and B, respectively from that of the base steel. On the other hand, the increment of tensile strength by the single addition of Mo was 40 MPa and lower than that by the single addition of Nb although the tensile strength of Mo–B steel was the same level as that of Nb–B steel.

3.1.2. Microstructure Observation of Rolling Plates

Scanning electron micrographs of six tested steels are shown in **Fig. 3**. The microstructure and morphology of bainite of Nb steel, Mo steel and B steel were different from those of Nb–B steel and Mo–B steel. Ferrite with little cementite in a grain, was dominant in the microstructure of the base steel with the tensile strength of 410 MPa as indicated in Fig. 1. In Mo steel, much ferrite and a little bainite were formed. Deformed ferrite and bainite were formed in B steel. This result indicates that this steel was rolled in the non-recrystallization region. Bainite fraction in B steel was larger than that in the base and Mo steels. Deformed fine ferrite and bainite were formed in Nb steel. This result indicates that total reduction in the non-recrystallization area increases in Nb steel. Fine bainite, which had laths partially, was formed in Nb–B and Mo–B steels. These fine microstructures affected the balance of strength and low temperature toughness as indicated in Fig. 1. Bainite fraction in Nb–B and Mo–B steels were higher than that of Nb steel. These microstructures of the combined addition affected the tensile strength indicated in Fig. 1. From these results, the combined addition of Nb and B or that of Mo and B was very effective for achieving high strength and high toughness. The combined additions were the concept to obtain a good balance of tensile strength and low temperature toughness on utilizing low C- B bearing steels.

3.1.3. α-Ray Track Etching (ATE)

Figure 4 shows the distribution of B in plates revealed by ATE method. B along the ferrite grain boundaries was recognized in B steel. On the other hand, B along the elongated prior γ grain boundaries was recognized in Nb–B and Mo–B steels. Elongated γ grains were observed in Nb–B and Mo–B steels. On the other hand, few elongated grains in B steel were observed. B was observed along the ferrite

grain boundary and was found in coarse precipitates in B steel. These results indicated that the segregated B in γ grain boundary suppressed ferrite transformation and resultantly developed bainitic microstructure, that is, it contributed to the increase in hardenability.

3.1.4. B Content from Electrolytic Extraction Residue

Table 2 shows B content measured on residue prepared by electrolytic extraction. B content in residue was 2.1 ppm in B steel and was out of detection in Nb–B and Mo–B steels respectively (<0.5 ppm). A lot of B precipitates existed in B steel, however, almost no B precipitates were formed in Nb–B and Mo–B steels. However, fine B precipitates less than 0.2 μm might not be collected in the electrolytic extraction residue.

3.1.5. TEM Observation

Figure 5 shows the transmission electron micrographs of extraction replica for B bearing steels. Precipitates shown in this figure were identified using EDS and electron beam diffraction patterns. The constitution and distribution of precipitates of B steel were different from those of Nb–B and Mo–B steels. The fine cementites precipitated along the prior γ grain boundaries in the Nb–B and Mo–B steels. On the other hand, a large amount of coarse cementite precipitates in B steel, that is, the formation of the coarse cementite was suppressed by the combined addition of Nb and B or that of Mo and B. Moreover, a lot of $Fe_{23}(C,B)_6$ precipi-

Table 2. Boron content measured from residual generated of electrolytic extraction in 20 mm thick plate.

B steel	2.1ppm
Nb-B steel	<0.5ppm
Mo-B steel	<0.5ppm

Note) 0.2 μm mesh

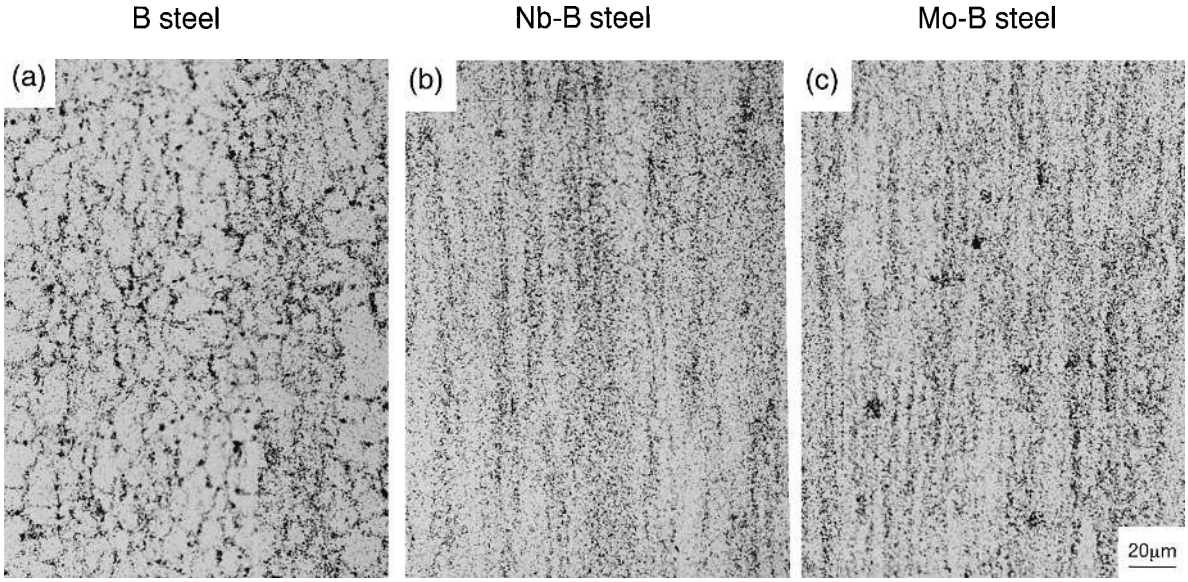

Fig. 4. ATE images of 20 mm thick plates.

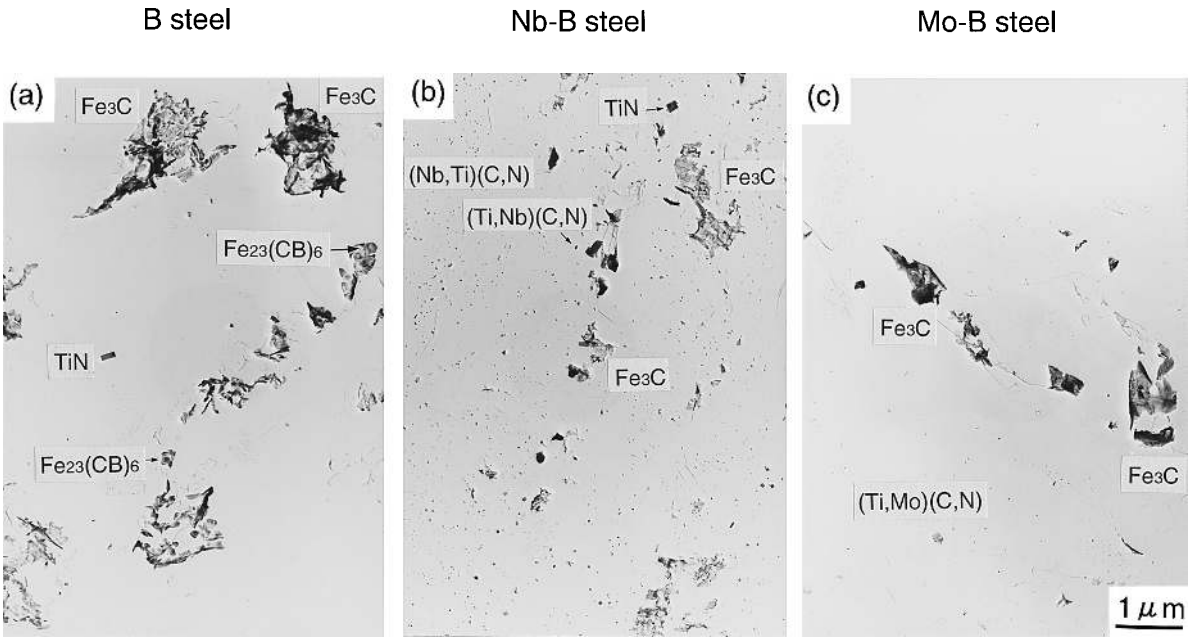

Fig. 5. TEM images of extraction replica of 20 mm thick plates.

tate was observed in B steel. However, no $Fe_{23}(C,B)_6$ precipitate was observed in Nb–B and Mo–B steels. TiN and fine dispersive precipitates with about 10 to 30 nm in length along the prior γ grain boundaries or in the prior γ grains were observed in Nb–B and Mo–B steels. The precipitates in Nb–B steel were identified as Nb(C,N), (Nb,Ti)(C,N) and those in Mo–B steel were identified as Ti(C,N) and (Ti,Mo)(C,N). TiN also precipitated in B steel.

3.1.6. AP-FIM Observation

FIM observation was carried out in order to investigate the ultra fine precipitates which were not be able to be detected by TEM. The FIM images of complex precipitates of TiN and Nb(C,N) in Nb–B added steel are shown in **Fig. 6**. The size of complex precipitates of TiN and Nb(C,N) were the same as that observed in TEM. The TiN were also observed in B and Mo–B steels using FIM. **Figure 7** shows the FIM images of B, Nb–B and Mo–B steels. Two continuous images in Mo–B steel were taken by using field evaporation method.[22] The ultra fine dispersive precipitates less than 1 to 3 nm were observed in Mo–B steels. Four precipitates were formed in FIM image in Mo–B steel, on the other hand, fine precipitates similar to that observed in Nb–B steel were confirmed in the center of FIM image. These precipitates were identified as metal (Nb or Mo)–C cluster by AP analysis.

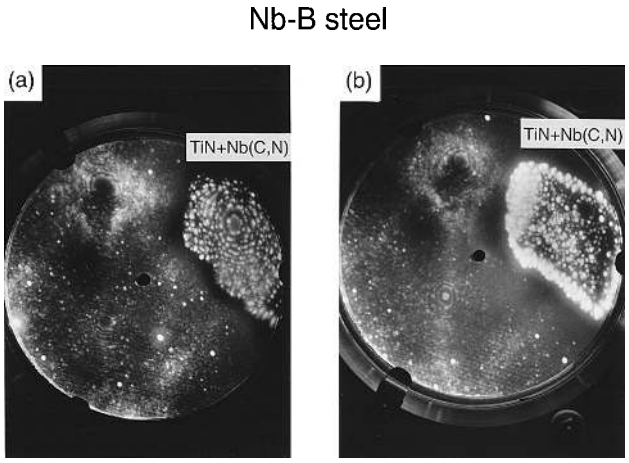

Fig. 6. FIM images of complex precipitates of TiN+Nb(C,N).

3.2. Transformation Behavior after Hot Working Using Hot-rolling Simulator

Transformation behavior after hot working using hot-rolling simulator was investigated in B bearing steels in order to confirm whether B precipitates in the γ region in B steel or not as compared with γ to α transformation behavior of 20 mm thick plates.

3.2.1. Effect of Cooling Rate on Transformation Behavior

The effect of cooling rate on transformation temperature of B, Nb–B and Mo–B steels after hot-working at 850°C is indicated in **Fig. 8**. The γ to α transformation temperature decreased with increasing cooling rate. The γ to α transformation temperature of B steel was higher than that of Nb–B and Mo–B steels at any cooling rate. The γ to α transformation temperature of Nb–B steel was higher than that of Mo–B steel. Hardness of B steel was the lowest and that of Mo–B steel was the highest of all B bearing steels at any cooling rates. Hardness had a large dependence on chemical composition and also on a cooling rate at 10°C/s or higher. Hardness did not depend on a cooling rate at 10°C/s

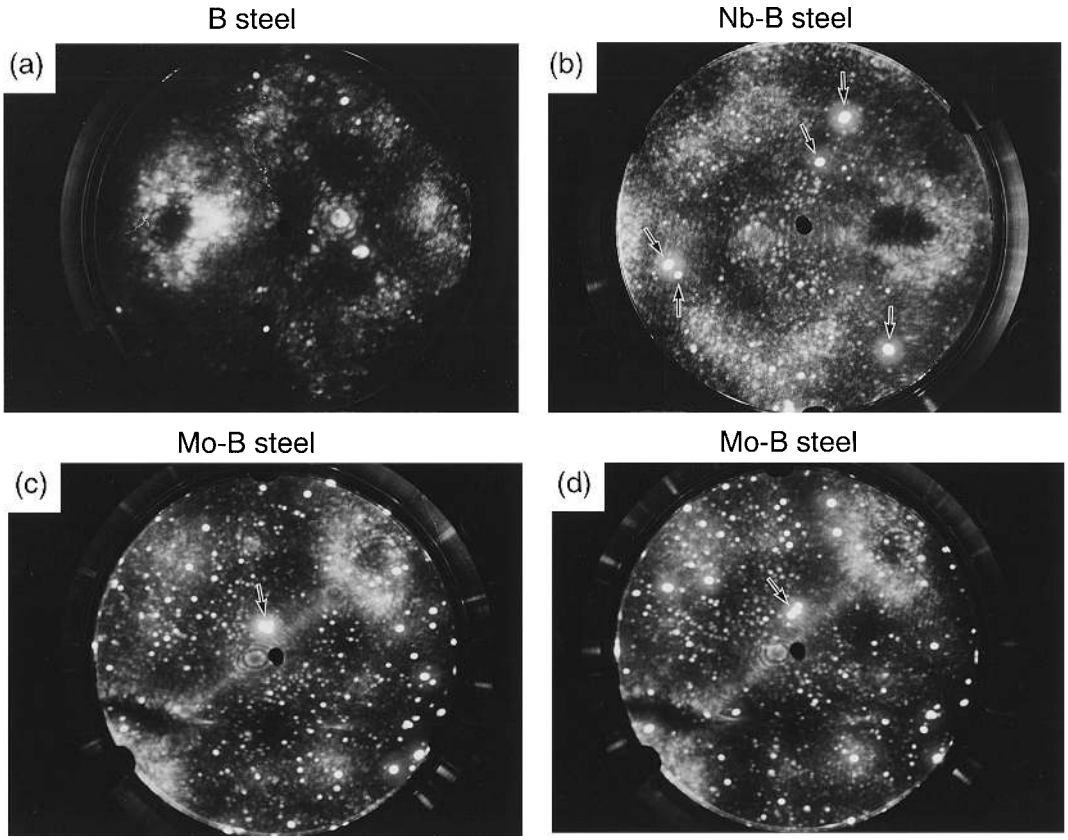

Fig. 7. FIM images showing the soluble atoms and ultra-fine precipitates (M–C cluster).

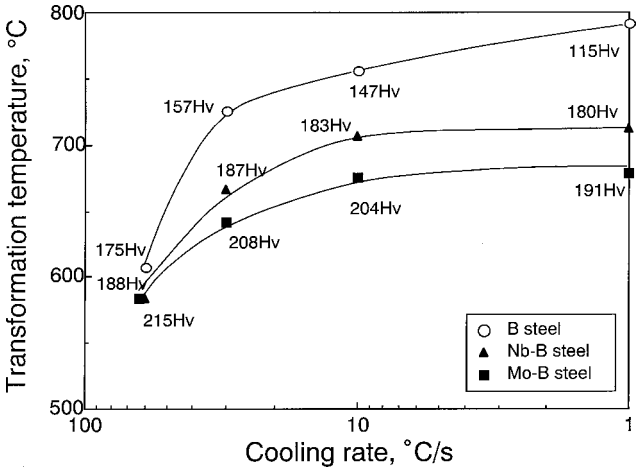

Fig. 8. Effect of cooling rate on transformation temperature.

or lower.

3.2.2. Microstructure Observation

SEM images of B, Nb–B and Mo–B steels cooled by He gas after hot working at 850°C are shown in **Fig. 9**. Bainite single phase was observed in all steels, that is, no ferrite phase was formed. Optical micrographs of these steels cooled at 10°C/s were indicated in **Fig. 10**. Bainite single phase was observed in Nb–B and Mo–B steels cooled at 10°C/s, although ferrite phase was partially formed in B steel. The microstructure cooled at 10°C/s indicated in Fig. 10 was similar to that of 20 mm thick rolled plates indicated in Fig. 1. The hardness results cooled at 10°C/s was also close to the tensile strength of 20 mm plates as mentioned before.

3.2.3. α-ray Track Etching (ATE)

ATE images of B bearing steels cooled by He gas were

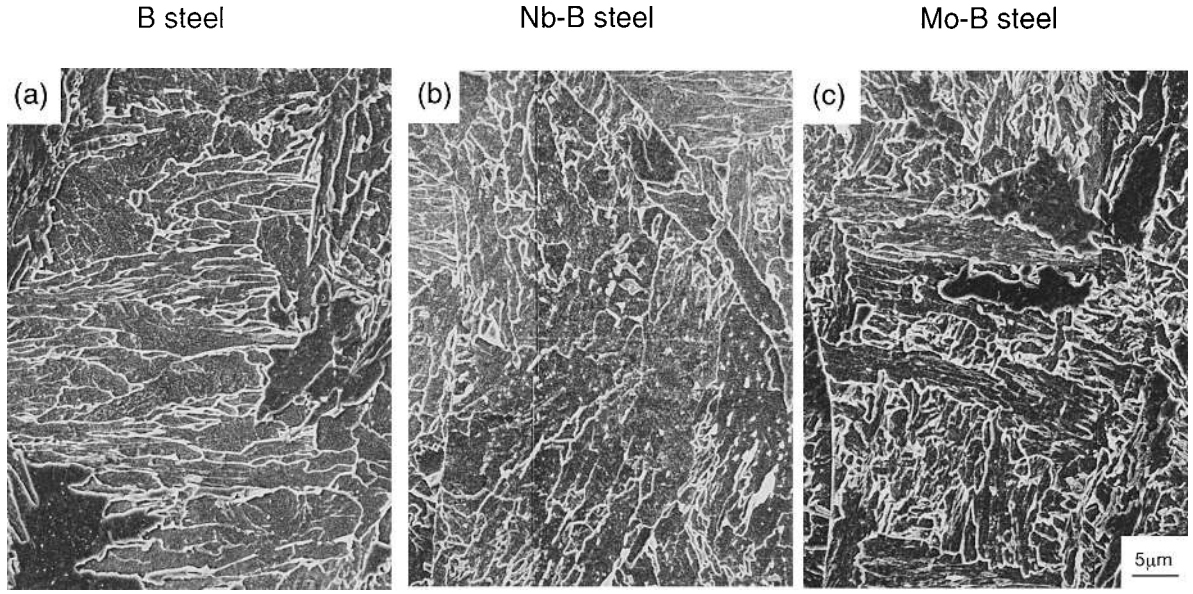

Fig. 9. Scanning electron micrographs quenched by He gas after hot working at 850°C.

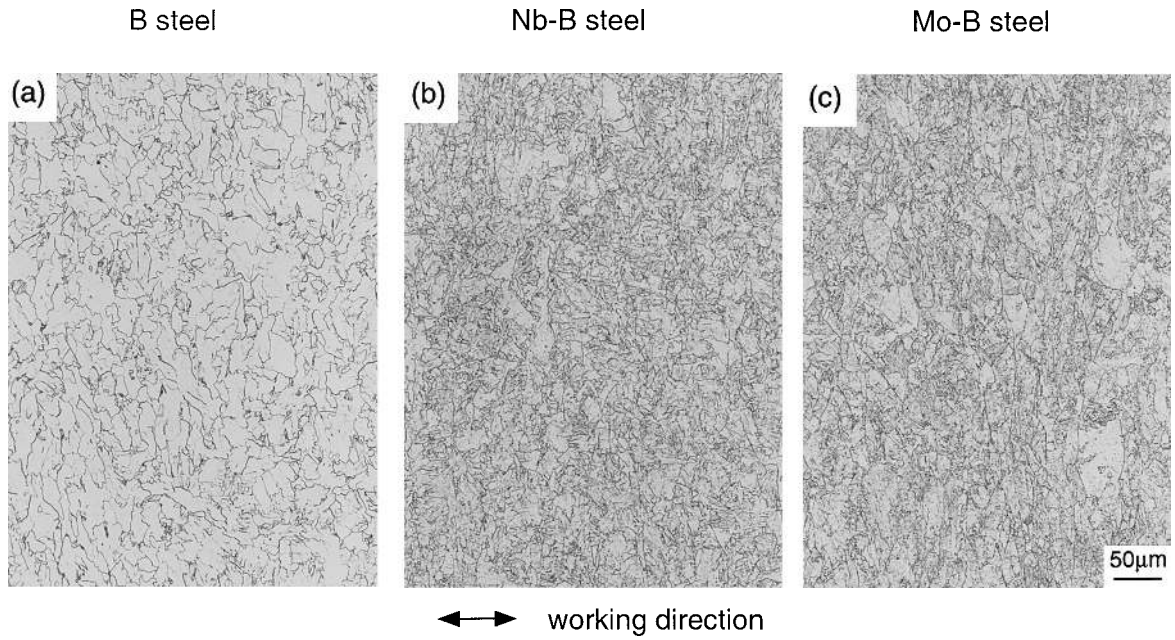

Fig. 10. Optical micrographs cooled at 10°C/s hot working at 850°C.

investigated in order to evaluate the segregation of B in γ region. **Figure 11** shows the distribution of B revealed by the ATE method in B, Nb–B and Mo–B steels cooled by He gas after hot working at 850°C. B segregated along the prior γ grain boundary in Nb–B and Mo–B steels. On the other hand, B was found in coarse precipitates in B steel as indicated by the arrows, while the segregated B along the elongated prior γ grain boundaries was recognized. This result showed that a lot of B precipitates were formed in the γ region in B steel. This result indicates that the segregated B along the γ grain boundary affected to the γ to α transformation behavior and the microstructures.

3.2.4. B Content from Electrolytic Extraction

Table 3 shows B content measured in residue prepared by electrolytic extraction. B content was 1.0 ppm in B steel and was out of detection in Nb–B and Mo–B steels respectively ($<$0.5 ppm). B precipitates existed in B steel, however, B precipitates were not almost formed in Nb–B and Mo–B steels. The B precipitate contents measured for specimens cooled by He gas were smaller than that measured from 20 mm thick plates in B steel. This result indicates that some of B precipitates were formed after the γ to α transformation.

3.2.5. TEM Observation

Figure 12 shows the transmission electron micrographs of extraction replica in B steel cooled by He gas after hot working at 850°C. A lot of precipitates whose size was 0.2 μm were observed. That is, these precipitates were formed along the prior γ grain boundary. These precipitates were identified as $Fe_{23}(C,B)_6$ from diffraction patterns. However, no $Fe_{23}(C,B)_6$ was observed in Nb–B and Mo–B

Table 3. Boron content measured from residual generated of electrolytic extraction in quenched by He gas from austenite region.

B steel	1.0ppm
Nb-B steel	<0.5ppm
Mo-B steel	<0.5ppm

Note) 0.2 μm mesh

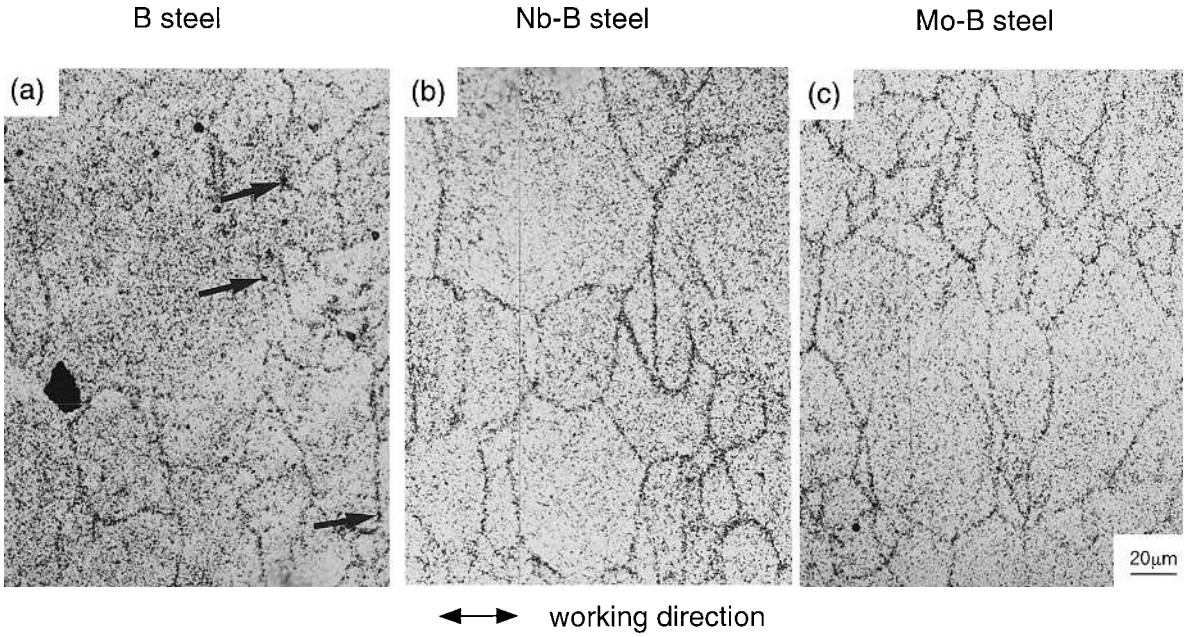

Fig. 11. ATE images quenched by He gas after hot working at 850°C.

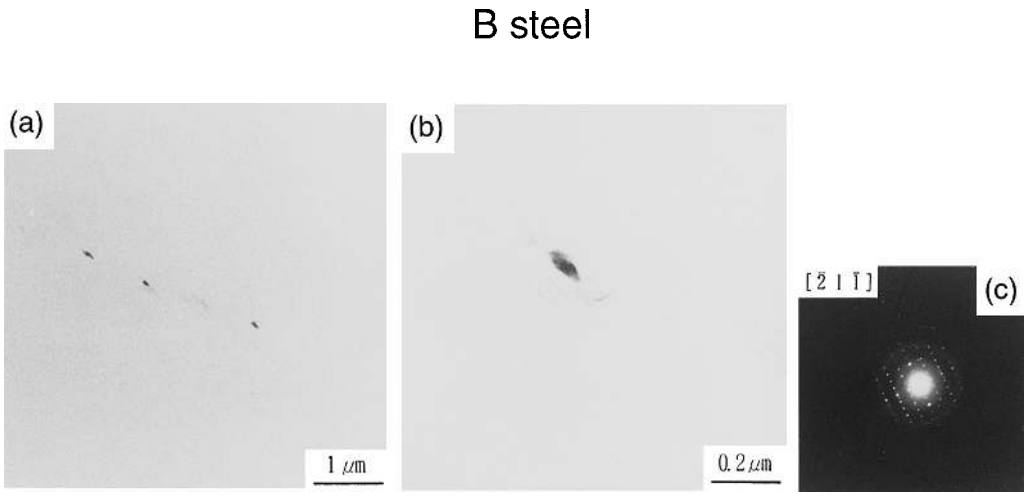

Fig. 12. TEM images of extraction replica quenched by He gas after hot working at 850°C.

steels. It was shown that a lot of B precipitates in the γ region in B steel as shown in 3.2.3. $Fe_{23}(C,B)_6$ formed in the γ region decreased the B segregated along the γ grain boundary. The segregated B along the γ grain boundary was lowered, as a result, promoted the ferrite transformation in B steel.

4. Discussions

4.1. Effect of the Segregated B on the Bainite Transformation

Strength increased remarkably by the combined addition of Nb and B or that of Mo and B in 20 mm thick plates. This result is supported by the microstructure indicated in Fig. 3 and γ to α transformation behavior indicated in Fig. 8. This result is attributed to the retardation of γ to α transformation, that is, the promotion of bainite transformation. The mechanism of the retardation of γ to α transformation by the combined additions was considered. It is thought that the increase in the segregated B content in the γ region retards the γ to α transformation because the segregated B along the γ grain boundary in Nb–B and Mo–B steels seems to distribute more largely than that of B steel. A lot of coarse B precipitates were formed in B steel, however, coarse B precipitates along the prior γ grain boundary were not observed in the combined additions in the ATE images. The precipitated B content measured on the residue prepared by the electrolytic extraction decreased markedly due to the combined additions. From TEM observation, these B precipitates were identified as $Fe_{23}(C,B)_6$ in B steel. Therefore, the formation of $Fe_{23}(C,B)_6$ along the γ grain boundary was suppressed by the combined additions, as a result, the segregated B along the prior γ grain boundary increased.

4.2. B Distribution in B Steel

Bainite transformation occurred, that is, grain boundary ferrite was not formed because almost all B segregated in the γ grain boundary in case of combined additions. Therefore, B segregated only along the prior γ grain boundary that was ferrite grain boundary in the combined addition steels. On the other hand, a lot of B precipitates were formed along the ferrite grain boundary in 20 mm thick plate of B steel. As shown before, B existed along the ferrite grain boundary, however, a lot of B and some B precipitates existed along the γ grain boundary for a rapid cooled specimen of hot rolling simulation. These results indicate that the segregated B along the γ grain boundary in B steel was smaller than that in the combined addition steels. As the results, the grain boundary ferrite was formed because γ to α transformation was not suppressed by B in B steel. The segregated B in γ grain boundary moved to the α grain boundary because prior γ grain boundary disappeared by the nucleation and growth of grain boundary ferrite and B precipitates were formed along the α grain boundary during cooling after γ to α transformation. These suggest that a lot of B segregated dominantly along γ grain boundary during γ region in case of B steel.

Therefore, it is necessary to confirm whether B precipitated in the γ region in B steel or not. For the steels cooled by He gas from γ region, no ferrite phase was formed, that is, bainite single phase were formed in all the steels. The γ to α transformation temperature for B steel was 20°C higher than that of Nb–B and Mo–B steels. That is, the γ to α transformation was retarded by the combined additions. No $Fe_{23}(C,B)_6$ in the γ region were formed in Nb–B and Mo–B steels. On the other hand, $Fe_{23}(C,B)_6$ were formed along the prior γ grain boundary in B steel cooled by He gas after hot working from TEM observation of extraction replica (Fig. 12) and the ATE image (Fig. 11). Moreover, the precipitated B content of B steel cooled by He gas after hot working at 850°C was 1.0 ppm, although that of Nb–B and Mo–B steels were less than the detection limit in the same condition as that of B steel. This result corresponds to TEM observation. That is, $Fe_{23}(C,B)_6$ was formed in the γ region in B steel. In other words, the formation of $Fe_{23}(C,B)_6$ in the γ region was suppressed by the combined additions, as a result, the segregated B along the γ grain boundary increased.

4.3. Effect of Combined Additions on B Precipitates in Combined Additions

The reason why the formation of $Fe_{23}(C,B)_6$ was suppressed in γ region by the combined additions is considered. Reducing C content is effective for suppressing the formation of $Fe_{23}(C,B)_6$. That is, $Fe_{23}(C,B)_6$ content increases with increasing C content because the driving force of nucleation is drastically elevated. In the present study, C content is 0.015% and the same in B steel , Nb–B steel and Mo–B steel.

From the results of TEM observation, the fine dispersive precipitates such as (Nb,Ti)(C,N) or (Ti,Nb)(C,N) were formed by the combined addition of Nb and B. In AP-FIM observation, the ultra fine dispersive precipitates such as Nb–C cluster were observed. On the other hand, due to the combined addition of Mo and B, (Ti,Mo)(C,N) and Mo–C clusters were observed in 20 mm thick plates. The fine carbide precipitates and C clusters are easy to be formed because Mo and C, as well as Nb and C, have a strong affinity. From these results, the reason why the formation of $Fe_{23}(C,B)_6$ was suppressed by the combined additions is thought that C precipitates and C clusters by the additions of Nb and Mo retard the C diffusion to the γ grain boundary. As a result, the formation of $Fe_{23}(C,B)_6$ was suppressed because the segregation of C along the γ grain boundary was suppressed. Tanaka *et al.*[24] has already reported that the diffusion rate of C at 900°C or lower was lowered by the addition of Nb and Mo in 0.1% C steel.

4.4. Relationship between Segregated B and C Precipitates in Combined Additions

It is necessary to indicate whether the precipitates such as Nb and Mo carbide or Nb–C and Mo–C cluster were formed in the γ region. At first, the relationship between the interaction of Nb–C and the segregated B along the grain boundary and that of Mo–C and the B segregated was considered. It is necessary to consider the interaction behavior of Nb and C or that of Mo and C in the γ region at temperatures from γ to α transformation temperature to 1 200°C. The effect of heating temperature on the solute Nb content was calculated by the equation of Irvine *et al.*[25] It is assumed that all nitrogen content is fixed with Ti. Nb(C,N) begins to precipitate less than 960°C. It is easy to form the Nb–C cluster or Nb(C,N) during hot rolling

because Nb and C have a strong affinity as mentioned above. Actually, Nb–C cluster or Nb precitipates, such as (Nb,Ti)(C,N) or (Ti,Nb)(C,N), were observed in TEM or AP-FIM. This leads to that C diffusion toward the γ grain boundary reduced, as a result, the formation of $Fe_{23}(C,B)_6$ was depressed because of the reduced C content in solution.

Mo carbonnitride is supposed to precipitate less than 900°C.[26] Mo–C cluster or Mo carbonnitride during hot rolling or before γ to α transformation is easy to precipitate because Mo and C, as well as Nb and C, have a strong affinity. Actually, Mo–C cluster and (Ti,Mo)(C,N) were observed in TEM and AP-FIM. C diffusion to the γ grain boundary were suppressed because Mo-cluster and Mo carbonnitride were formed.

There might be another reason why the formation of $Fe_{23}(C,B)_6$ in the γ region was suppressed by the combined addition of Nb and B and that of Mo and B because Nb and Mo are soluble above 960°C.[25,26] It is possible for C contents supplied to the γ grain boundary to be reduced because Nb and C or Mo and C have a strong affinity even in the temperature range from 960 to 1 200°C.

4.5. Mechanism of Improvement of Hardenability by the Combined Additions

The mechanism of the improvement of hardenability by the combined additions was considered. The increase in the segregated B along γ grain boundary retards γ to α transformation. In other words, the increase in the segregated B decreases γ to α transformation temperature. The segregated B along γ grain boundary decreases if B precipitates are formed there because of the excessive B segregation. Therefore, the formation of B precipitates along γ grain boundary accelerates γ to α transformation.

Three factors to suppress the formation of B precipitates which is $Fe_{23}(C,B)_6$ are considered. The effectiveness for the suppression of formation of $Fe_{23}(C,B)_6$ is (1) the decrease in C content, (2) the suppression of segregated C along the γ grain boundary due to the retardation of C diffusion by the C precipitates or C cluster during rolling, and (3) the depression of the segregated C along γ grain boundary during reheating.

The difference in the hardenability by the combined addition was discussed in Nb–B and Mo–B steels. The increase in tensile strength per Nb atomic weight percent in Nb–B steel (4 900 MPa/at%) was approximately 8 times higher than that in Mo–B steel (630 MPa/at%) because Mo content for atomic weight was 10 times higher than Nb content for atomic weight, and the increases in tensile strength in Nb–B and Mo–B steel were 120 and 130 MPa, respectively being almost the same. It is reasonable that the suppression of $Fe_{23}(C,B)_6$ is due to the decrease in the segregated C content along the γ grain boundary by the retardation of C diffusion due to the formation of the C precipitates and C clusters, considering that the increase in hardenability due to the combined addition of Nb and B is 8 times higher than that of Mo and B and considering that C precipitates and C clusters were formed in Nb–B much larger than in Mo–B steel as indicated from TEM observation (Fig. 5).

From these results, it is suggested that the lowering of C diffusion towards the γ grain boundary due to the formation of C precipitates and C cluster suppressed the formation of $Fe_{23}(C,B)_6$ along the γ grain boundary by the combined additions, as the results, the segregated B along the γ grain boundary increased.

Reduced C content in solution due to the precipitation of Nb or Mo carbide and Nb and Mo clusters did increase hardenbility in B bearing steels. In other words, the γ to α transformation was retarded because of the suppression of C diffusion toward the γ grain boundary by lowering C content in B bearing steels. It is thought that lowering C content is equivalent to the suppression of C diffusion towards the γ grain boundary because carbide or C cluster precipitate due to the combined addition of Nb and B or that of Mo and B.

Finally, in the present study, it was not observed that the direct interaction of Mo and B or that of Nb and B affect the suppression of $Fe_{23}(C,B)_6$. The mechanism of suppress-

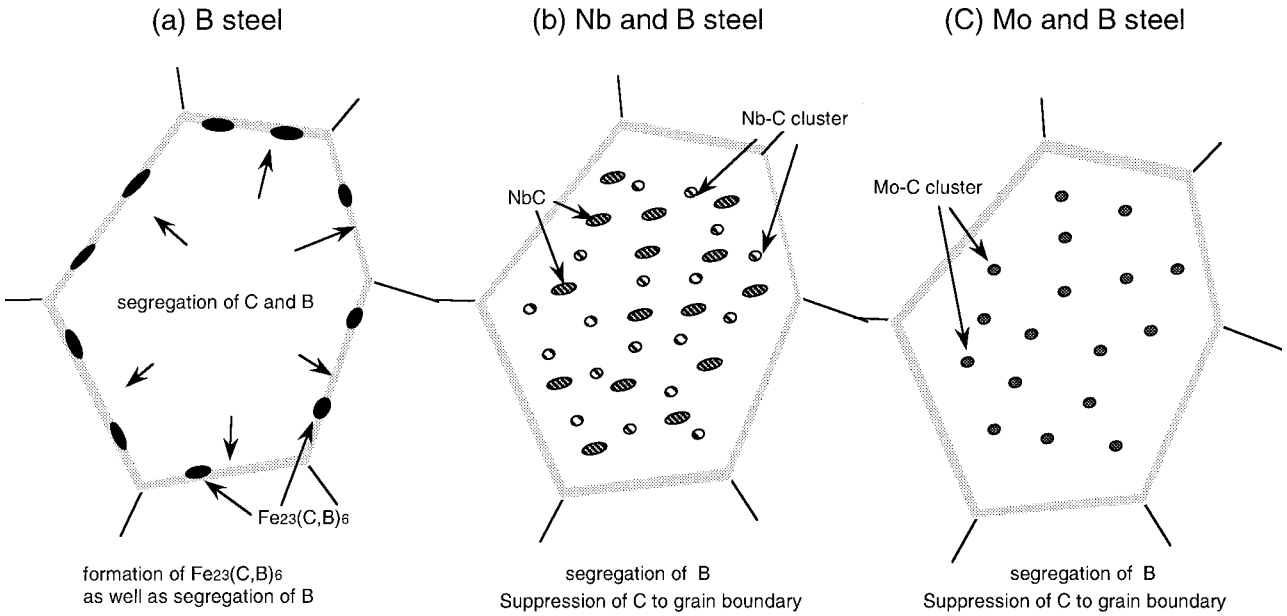

Fig. 13. Schematic diagram showing mechanism for suppression of formation of $Fe_{23}(C,B)_6$ due to combined addition of Nb and B or Mo and B.

ing $Fe_{23}(C,B)_6$ is schematically indicated in **Fig. 13**.

(1) B single addition: B as well as C segregated in γ grain boundary and $Fe_{23}(C,B)_6$ were partially formed (Fig. 13(a)).

(2) Combined addition of Nb and B: The reason of the suppression of $Fe_{23}(C,B)_6$ by the combined addition is that the supplement of C contents to the γ grain boundary was suppressed by the precipitation of Nb–C clusters or Nb carbonnitride (Fig. 13(b)).

(3) Combined addition of Mo and B: The reason of the suppression of $Fe_{23}(C,B)_6$ by the combined addition is that the supplement of C contents to the γ grain boundary was suppressed by the precipitation of Mo–C clusters or Mo carbonnitride (Fig. 13(c)).

Therefore, since the formation of $Fe_{23}(C,B)_6$ is suppressed by the combined additions, as a result, the segregated B along the γ grain boundary increased. Then, γ to α transformation was retarded and hardenability increased due to the combined additions.

5. Conclusions

The mechanical properties of the combined additions of Nb and B and that of Mo and B in the low C steels and the mechanism of increase in hardenability by the combined additions were investigated. The main conclusions were as follows. The strength remarkably increases due to the combined addition of Nb and B or that of Mo and B because γ to α transformation is retarded, that is, bainite transformation is promoted. This is caused by the increase in the segregated B along the γ grain boundary before γ to α transformation. The mechanism is attributed to the suppression of the formation of $Fe_{23}(C,B)_6$ precipitates by the combined additions because C diffusion towards the γ grain boundary is suppressed due to the precipitation of the fine dispersive (Nb,Ti)(C,N) and the formation of C clusters of Nb and Mo during rolling or during cooling after rolling in γ region.

REFERENCES

1) Ph. Maitrepierre, J. Rofes-Vernis and D. Thivellier: Boron in Steel, ed. by S. K. Banerji and J. E. Morral, AIME, Warrendale, PA, (1979), 1.
2) R. A. Grange and J. B. Mickel: *Trans. Am. Soc. Met.*, **53** (1956), 157.
3) B. M. Kapadia, R. M. Brown and W. J. Murphy: *Trans. TMS-AIME*, **242** (1968), 1969.
4) M. Ueno and T. Inoue: *Trans. Iron Steel Inst. Jpn.*, **13** (1973), 210.
5) G. F. Melloy, P. R. Slimon and P. P. Podgursky: *Metall. Trans.*, **4** (1973), 2279.
6) A. Brown, J. D Garnish and R. W. K. Honeycombe: *Met. Sci.*, **8** (1974), 317.
7) Y. Yamanaka and Y. Ohmori: *Trans. Iron Steel Inst. Jpn.*, **17** (1977), 92: **18** (1978), 492.
8) R. Habu, M. Miyata and S. Sekino and S. Goda: *Trans. Iron Steel Inst. Jpn.*, **18** (1978), 492.
9) K. Terasawa, H. Higashiyama and S. Sekino: Toward Improved Ductility and Toughness, Climax Molybdenum Development Company, Japan, (1971), 103.
10) A. Massip and L. Meyer: *Stahl Eisen*, **98** (1978), 989.
11) H. Nakasugi, H. Matsuda and H. Tamehiro: Alloys for the 80's, Climax Molybdenum, Ann Arbor, (1980).
12) K. Matsumoto, T. Taira, K. Ume, T. Hyodo, K. Tsukada and K. Arikata: *Tetsu-to-Hagané*, **69** (1983), S1350; *Trans. Iron Steel Inst. Jpn.*, **24** (1984), B92.
13) T. Hashimoto H. Ohtani M. Nakanishi, Y. Komizo and Y. Fujishiro: *Tetsu-to-Hagané*, **69** (1983), A309.
14) H. Tamehiro, M. Murata, R. Habu and M. Nagumo: *Trans. Iron Steel Inst. Jpn.,* **27** (1987), 120.
15) L. Karlsson and H. Norden: *Acta Metall.*, **36**, (1988), No. 1, 35.
16) H. Asahi, M. Ueno and H. Fujii: *CAMP-ISIJ*, **7** (1994), 853.
17) H. Asahi: *CAMP-ISIJ*, **11** (1998), 482.
18) H. Asahi: *ISIJ Int.*, **42** (2002), No. 10, 1150.
19) C. P. Beam, R. L. Fleischer, P. W. Swart and H. R. Hart: *J. Appl. Phys.*, **37** (1996), 2218.
20) J. D. H. Hughs and G. T. Rogers: *J. Inst. Met.*, **95** (1967), 299.
21) J. S. Armjo and H. S. Osenbaum: *J. Appl. Phys.*, **38** (1967), 2064.
22) R. Uemori and M. Tanino: *Bull. Jpn. Inst. Met.*, **25** (1986), 222.
23) R. Uemori, M. Saga and H. Morikawa: *Bull. Jpn. Inst. Met.*, **30** (1991), 498.
24) T. Tanaka and S. Enokinami: *Tetsu-to-Hagané*, **58** (1972), 1775.
25) K. J. Irvine, F. B. Pickering and T. Gladman: *J. Iron Steel Inst.*, **205** (1967), 161.
26) H. Morikawa and T. Sato: Proc. of 5th Int. Conf. on High Voltage Electron Microscopy, Japanese Society of Electron Microscopy, Japan, (1977), 531.
27) L. Karlsson and H. Norden: *Acta Metall.*, **36** (1988), No. 1, 13.
28) R. Uemori and H. Morikawa: *Hyoumengizyutu*, **42** (1991), No. 1, 62.